Chinese Journal of Aeronautics, (2014),27(4): 875–883

Chinese Society of Aeronautics and Astronautics
& Beihang University

Chinese Journal of Aeronautics

cja@buaa.edu.cn
www.sciencedirect.com

A guidance law for UAV autonomous aerial refueling based on the iterative computation method

Luo Delin [a,*], Xie Rongzeng [a], Duan Haibin [b]

[a] *Department of Automation, Xiamen University, Xiamen 361005, China*
[b] *State Key Laboratory of Virtual Reality Technology and Systems, Beihang University, Beijing 100191, China*

Received 28 July 2013; revised 9 September 2013; accepted 18 October 2013
Available online 4 July 2014

KEYWORDS

Autonomous aerial refueling;
Aerial rendezvous;
Formation control;
Guidance law;
Unmanned aerial vehicle

Abstract The rendezvous and formation problem is a significant part for the unmanned aerial vehicle (UAV) autonomous aerial refueling (AAR) technique. It can be divided into two major phases: the long-range guidance phase and the formation phase. In this paper, an iterative computation guidance law (ICGL) is proposed to compute a series of state variables to get the solution of a control variable for a UAV conducting rendezvous with a tanker in AAR. The proposed method can make the control variable converge to zero when the tanker and the UAV receiver come to a formation flight eventually. For the long-range guidance phase, the ICGL divides it into two sub-phases: the correction sub-phase and the guidance sub-phase. The two sub-phases share the same iterative process. As for the formation phase, a velocity coordinate system is created by which control accelerations are designed to make the speed of the UAV consistent with that of the tanker. The simulation results demonstrate that the proposed ICGL is effective and robust against wind disturbance.

1. Introduction

With the rapid development of UAV technologies, UAVs are being used to carry out various missions like high altitude surveillance and reconnaissance, long distance military strikes, etc., some of which require UAVs to continuously stay in the air for a quite long time. To this end, autonomous aerial refueling (AAR) becomes a key issue to be addressed for these applications of UAV. There are four main tasks to be accomplished sequentially during AAR of UAV: UAV rendezvous, formation maintaining, pipeline docking, and refueling. This paper mainly focuses on presenting a guidance law for the rendezvous and formation maintaining processes. For decades, a lot of achievements have been made to develop guidance technologies for the UAV rendezvous problem.[1–3] One of the most mature technologies is the classical proportional navigation guidance (PNG).[4] After that, many improved proportional

* Corresponding author. Tel.: +86 592 2580057.
E-mail addresses: luodelin1204@xmu.edu.cn (D. Luo), xierongzeng2013@163.com (R. Xie), hbduan@buaa.edu.cn (H. Duan).

Peer review under responsibility of Editorial Committee of CJA.

Production and hosting by Elsevier

http://dx.doi.org/10.1016/j.cja.2014.06.003
1000-9361

navigation guidance (IPNG) schemes have been evolved based on PNG.[5–7] To further enhance the guidance performance, modern control theories, such as sliding mode control,[8–10] differential geometric method,[11–13] neural network,[14–16] and so on, are also employed for the design of UAV rendezvous guidance laws. For formation maintaining, there are several existing methods. In Ref. 17, a full-state linearization via a dynamic feedback controller is designed for controlling two robots in a leader–follower configuration. In Ref. 18, a synchronized position tracking controller is incorporated in formation flight control for multiple flying wings. Ref. 19 proposed a new approach of hybrid supervisory control for the leader–follower formation problem. The hybrid supervisory control approach provides a tractable framework for hybrid synthesis of formation control. Within this framework, a new method of abstraction based on polar partitioning of the state space is introduced. Ref. 20 presented an iterative guidance method for launch vehicles. In this method, the guidance for a launch vehicle is formulated as an optimal control problem, in which the transient state of the vehicle is taken as the initial value and the target point as the terminal constraint. The objective function is to minimize the flight time of the vehicle moving from the current position to the target point. During the whole flight process of the vehicle, for each time interval, the control solution and the corresponding flying trajectory are obtained by solving the established guidance equations. Through a repeated iterative computation, the launch vehicle is eventually guided to the target point and satisfies its predefined state. This method has been studied for the guidance and control design of launch vehicles and ballistic missiles.[21–24] However, these approaches involve heavy computation load and are difficult for practical engineering applications.

In this paper, a novel iterative computation guidance law (ICGL) is proposed for a UAV to perform rendezvous and formation maintaining with a tanker in the AAR process. In the ICGL, the rendezvous process of a UAV with a tanker in AAR is divided into two major phases: the long-range guidance phase and the formation phase. In each phase, the ICGL computes the relative state parameters between the UAV and the tanker in real-time to obtain the specific control variable. Furthermore, the ICGL divides the long-range guidance phase into two sub-phases which share the same iterative process: the correction sub-phase and the guidance sub-phase. The ICGL proposed in this paper is totally different from the above mentioned iterative guidance method based on the optimal control theory. In the ICGL, a UAV approaches to a tanker along a smooth arc trajectory designed by a geometric method. Thus the iteration is based on the relative position between the UAV and the tanker in each time interval. The designed arc trajectory strategy has an advantage which makes the control vector perpendicular to the velocity of the UAV. Therefore, it is easy to be realized in practical engineering perspective.

The remainder of the paper is organized as follows. In Section 2, the problem of rendezvous for AAR is formulated mathematically. In Section 3, the ICGL algorithm is developed for a UAV to perform rendezvous and formation maintaining with a tanker in AAR. In Section 4, simulations are performed to verify the effectiveness of the proposed ICGL by comparing it with the nonlinear guidance (NG) method. Then simulation of wind disturbance injection is conducted to demonstrate the robustness of the ICGL. The conclusion remarks are given in Section 5.

2. Problem description

An illustrative diagram for the rendezvous process of a UAV with a tanker for aerial refueling is given in Fig. 1. The research objective of this paper is to guide the UAV near the tanker and then the UAV keeps a formation flight with the tanker.

In the UAV guidance process, there exist two situations for the relationship of the initial velocity between the UAV and the formation location: the unparallel one and the parallel one. The system can be described in the Earth-fixed inertial frame O_cxyz representing a general unparallel situation shown in Fig. 2 with its origin at the initial location of the UAV denoted as O_c. The orientation of the x-axis is consistent with the initial velocity vector of the UAV. The z-axis is downward and perpendicular to the x-axis in the vertical plane. The y-axis is determined according to the right-hand rule. Point F stands for the formation location and point P is the projection point of F on the O_cxy plane. H is an intersection point at which PH is perpendicular to the x-axis. The transitional state of the UAV during the rendezvous process is shown in Fig. 3, in which m is the surface which passes the velocity $\boldsymbol{V}_U$ of the UAV and is parallel with the x-axis when the velocity of the UAV is unparallel with the O_cxy plane.

The position vector of the UAV is denoted as

$$\boldsymbol{P}_U = [x_U, y_U, z_U]^T$$

The velocity vector of the UAV is

$$\boldsymbol{V}_U = \left[v_{Ux}, v_{Uy}, v_{Uz}\right]^T$$

The motion of the UAV can be described by the following kinematics equations[24]

$$\begin{cases} \dot{x}_U = v_U \cos\sigma \\ \dot{y}_U = v_U \sin\sigma\cos\gamma \\ \dot{z}_U = v_U \sin\sigma\sin\gamma \end{cases} \tag{1}$$

where v_U is the magnitude of $\boldsymbol{V}_U$ and

$$v_U = \sqrt{v_{Ux}^2 + v_{Uy}^2 + v_{Uz}^2} \tag{2}$$

σ is the angle between the velocity of the UAV and the x-axis. γ is the angle between the surface m and the O_cxy plane in the frame O_cxyz as shown in Fig. 3.

In Fig. 2, F is the tracking point for the UAV to keep a formation flight with the tanker. The location of F can be set according to the current position of the tanker with a deviation value $\Delta\boldsymbol{d}$ as shown in Fig. 2. The position vector of F can be expressed as

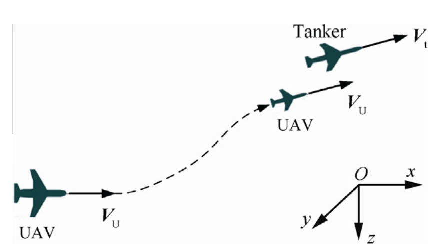

Fig. 1 An illustrative rendezvous process of a UAV with a tanker.

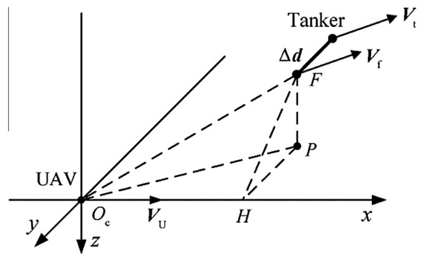

Fig. 2 Unparallel situation.

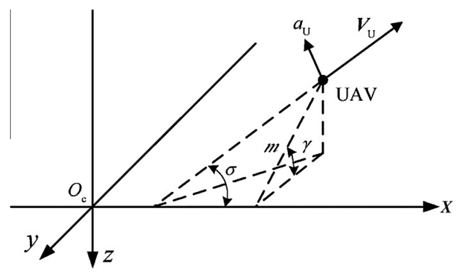

Fig. 3 State of the UAV during the guidance process.

$$\boldsymbol{P}_{\rm f} = \boldsymbol{P}_{\rm t} - \boldsymbol{\Delta d} = [x_{\rm f}, y_{\rm f}, z_{\rm f}]^{\rm T}$$

The velocity vector of F is

$$\boldsymbol{V}_{\rm f} = \boldsymbol{V}_{\rm t} = \left[v_{{\rm f}x}, v_{{\rm f}y}, v_{{\rm f}z}\right]^{\rm T}$$

where $\boldsymbol{P}_{\rm t}$ is the position vector of the tanker and $\boldsymbol{V}_{\rm t}$ is the velocity vector for the tanker.

The motion of F can be described by the following kinematics

$$\begin{cases} \dot{x}_{\rm f} = v_{{\rm f}x} \\ \dot{y}_{\rm f} = v_{{\rm f}y} \\ \dot{z}_{\rm f} = v_{{\rm f}z} \end{cases} \tag{3}$$

3. Design of guidance law

Since the parallel situation is an exceptional case of the unparallel one, the unparallel situation is mainly discussed in this paper. The rendezvous process can be divided into two phases: the long-range guidance phase and the formation phase.

3.1. Long-range guidance phase

The long-range guidance phase is defined from the initial instant to the instant when the distance between the UAV and F is equal to or smaller than a given value. When $\boldsymbol{V}_{\rm U}$ and $\boldsymbol{V}_{\rm f}$ are not parallel, the long-range guidance phase should also be further divided into two sub-phases: the correction sub-phase and the guidance sub-phase.

3.1.1. Correction sub-phase

The correction sub-phase is to adjust the direction of $\boldsymbol{V}_{\rm U}$ to be parallel with the velocity of the projection point P on the $O_{\rm c}xy$ plane firstly. The parallel situation is given in Fig. 4. The geometric relationship between the UAV and P in the $O_{\rm c}xy$ plane is shown in Fig. 5.

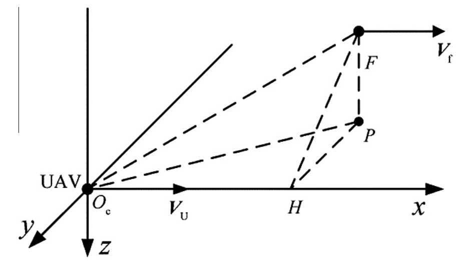

Fig. 4 Parallel situation.

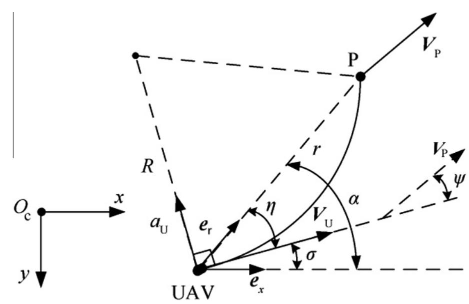

Fig. 5 Geometric relationship in the two-dimensional plane.

In Fig. 5, r is the distance between the UAV and P; α is the angle of line-of-sight from the UAV to P; η is the advance angle of the UAV; $\boldsymbol{V}_{\rm p}$ is the velocity of projection point P on the $O_{\rm c}xy$ plane; ψ is the angle between the velocities of the UAV and P; $\boldsymbol{e}_x$ is the unit vector of the x-axis and $\boldsymbol{e}_{\rm r}$ is the unit vector along the direction from the UAV pointing to P. The strategy used in this paper to guide the UAV from the initial position to location P is along an arc orbital approximation. The UAV can move along an arc trajectory from its current position to the target location P by applying a normal correction overload on the UAV.

The angle σ of the UAV satisfies the constraint

$$\dot{\sigma} = \frac{v_{\rm U}}{R}$$

where the radius of arc trajectory for the UAV moving to P can be calculated by

$$R = \frac{r}{2\sin\eta}$$

where $\eta = \alpha - \sigma$, in which $\alpha = \arccos\dfrac{\boldsymbol{e}_x \cdot \boldsymbol{e}_{\rm r}}{|\boldsymbol{e}_x||\boldsymbol{e}_{\rm r}|}$.

According to the analysis above, the control acceleration $a_{\rm U}$ can be calculated by

$$a_{\rm U} = \frac{v_{\rm U}^2}{R} \tag{4}$$

The iterative process throughout the correction sub-phase is shown below in detail.

(1) Initialization

Initialize the following parameters at the initial instant t_0:
The position vector of the UAV

$$\boldsymbol{P}_{\rm U}(t_0) = [x_{\rm U}(t_0), y_{\rm U}(t_0), z_{\rm U}(t_0)]^{\rm T} = [0, 0, 0]^{\rm T}$$

The velocity vector of the UAV

$$V_U(t_0) = [v_{Ux}(t_0), v_{Uy}(t_0), v_{Uz}(t_0)]^T = [v_U, 0, 0]^T$$

The position vector of P

$$P_p(t_0) = [x_p(t_0), y_p(t_0), z_p(t_0)]^T = [x_p, y_p, 0]^T$$

The velocity vector of P

$$V_p(t_0) = [v_{px}(t_0), v_{py}(t_0), v_{pz}(t_0)]^T = [v_{px}, v_{py}, v_{pz}]^T$$

The angle σ of the UAV

$$\sigma(t_0) = 0$$

The relative position vector of P to the UAV

$$r_{los}(t_0) = P_p(t_0) - P_U(t_0)$$

The magnitude of the distance between the UAV and P

$$r(t_0) = |r_{los}(t_0)|$$

The angle of line-of-sight

$$\alpha(t_0) = \arccos\frac{e_x \cdot r_{los}(t_0)}{|e_x||r_{los}(t_0)|}$$

The advance angle of the UAV

$$\eta(t_0) = \alpha(t_0) - \sigma(t_0)$$

The magnitude of the normal correction acceleration

$$a_U(t_0) = \frac{v_U^2}{R(t_0)} = \frac{2v_U^2 \sin\eta(t_0)}{r(t_0)}$$

(2) Iterative computation

In order to get a series of solutions for the control variable a_U using the iterative method, the differential equations in Eqs. (1) and (3) should be discretized by using the following formula

$$\dot{w}(t) = \frac{\partial w}{\partial t} = \frac{w(t+\Delta t) - w(t)}{\Delta t}$$

By this way, the guidance process can be divided into multiple discrete sub-processes as shown in Fig. 6. Each sub-process is regarded as a straight line motion with time interval Δt. Δs is the displacement of the UAV within interval Δt. $\Delta\beta$ is the correction angle of the UAV velocity after interval Δt.

From the discrete sub-processes, the value at each instant can be calculated step by step. Using i ($i = 1, 2, 3\ldots$) represent the ith iterative step, the iterative computation procedure can be illustrated as follows.

Step 1. Set $i = 1$ and $\gamma = 0$.

Step 2. Calculate the position vector of the UAV at t_i instant

$$P_U(t_i) = [x_U(t_i), y_U(t_i), z_U(t_i)]^T$$

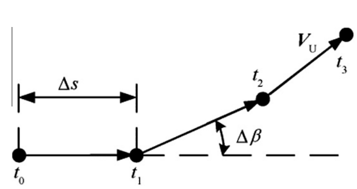

Fig. 6 Divided guidance process.

where

$$\begin{cases} x_U(t_i) = x_U(t_{i-1}) + v_{Ux}(t_{i-1})\Delta t \\ y_U(t_i) = y_U(t_{i-1}) + v_{Uy}(t_{i-1})\Delta t \\ z_U(t_i) = z_U(t_{i-1}) + v_{Uz}(t_{i-1})\Delta t \end{cases}$$

Step 3. Calculate the position vector of P at t_i instant

$$P_p(t_i) = [x_p(t_i), y_p(t_i), z_p(t_i)]^T$$

where

$$\begin{cases} x_p(t_i) = x_p(t_{i-1}) + v_{px}(t_{i-1})\Delta t \\ y_p(t_i) = y_p(t_{i-1}) + v_{py}(t_{i-1})\Delta t \\ z_p(t_i) = z_p(t_{i-1}) + v_{pz}(t_{i-1})\Delta t \end{cases}$$

Step 4. Update the velocity vector of P at t_i instant

$$V_p(t_i) = V_p(t_{i-1})$$

Step 5. Calculate the relative position vector of P to the UAV at t_i instant

$$r_{los}(t_i) = P_p(t_i) - P_U(t_i)$$

Step 6. Calculate the magnitude of the relative position vector of P to the UAV at t_i instant

$$r(t_i) = |r_{los}(t_i)|$$

Step 7. Calculate the angle of line-of-sight α at t_i instant

$$\alpha(t_i) = \arccos\frac{e_x \cdot r_{los}(t_i)}{|e_x||r_{los}(t_i)|}$$

Step 8. Update the angle σ of the UAV at t_i instant

$$\sigma(t_i) = \sigma(t_{i-1}) + \Delta\beta(t_{i-1})$$

Step 9. Calculate the velocity vector of the UAV at t_i instant

$$V_U(t_i) = [v_{Ux}(t_i), v_{Uy}(t_i), v_{Uz}(t_i)]^T$$

where

$$\begin{cases} v_{Ux}(t_i) = v_U \cos\sigma(t_i) \\ v_{Uy}(t_i) = v_U \sin\sigma(t_i) \\ v_{Uz}(t_i) = 0 \end{cases}$$

Step 10. Calculate the advance angle of the UAV at t_i instant

$$\eta(t_i) = \alpha(t_i) - \sigma(t_i)$$

Step 11. Calculate the magnitude of the UAV normal correction acceleration at t_i instant

$$a_U(t_i) = \frac{v_U^2}{R(t_i)} = \frac{2v_U^2 \sin\eta(t_i)}{r(t_i)}$$

Step 12. Calculate the correction angle of the UAV velocity at t_i instant

$$\Delta\beta(t_i) = \frac{a_U(t_i)}{v_U}\Delta t$$

Step 13. Calculate the angle between the velocity vectors of the UAV and P at t_i instant

$$\psi(t_i) = \arccos\frac{V_U(t_i) \cdot V_p(t_i)}{|V_U(t_i)||V_p(t_i)|}$$

Step 14. If $\psi(t_i)$ is smaller than a given value of 0.0005 rad in this paper, terminate the iterative computation and go into the guidance sub-phase. Otherwise, let $i = i + 1$, and go to step 2.

3.1.2. Guidance sub-phase

At the end of the correction sub-phase, the guidance sub-phase is activated. At the same instant the position relationship between the UAV and F as well as P in the frame $O_c xyz$ is shown in Fig. 7.

The position vector of F in Fig. 7 is

$$\boldsymbol{P}_f = [x_f, y_f, z_f]^T$$

where $x_f = x_p$, $y_f = y_p$, $z_f = z_d$, z_d is the required position component.

The velocity vector of F

$$\boldsymbol{V}_f = \boldsymbol{V}_p$$

In order to use the iterative computation algorithm similar to that used in the correction sub-phase, a coordinate system $O_g x'y'z'$ is created with its origin at the current location of the UAV. In the frame $O_g x'y'z'$, the orientation of the x'-axis is consistent with the current velocity direction of the UAV. The z'-axis is downward and perpendicular to the x'-axis in the vertical plane. The y'-axis can be determined according to the right-hand rule as shown in Fig. 7. The coordinate transformation from the frame $O_c xyz$ to the frame $O_g x'y'z'$ can be obtained by

$$\boldsymbol{P}' = \boldsymbol{R}_{gc}\boldsymbol{P} + \boldsymbol{D} \tag{5}$$

where $\boldsymbol{P}$ is a 3×1 position vector in the $O_c xyz$, P' is the transformed position vector in the $O_g x'y'z'$. $\boldsymbol{R}_{gc}$ is the rotation matrix from the frame $O_c xyz$ to the frame $O_g x'y'z'$ which can be calculated as follows:

$$\boldsymbol{R}_{gc} = \begin{bmatrix} \cos\sigma_{og} & \sin\sigma_{og} & 0 \\ -\sin\sigma_{og} & \cos\sigma_{og} & 0 \\ 0 & 0 & 1 \end{bmatrix} \tag{6}$$

where σ_{og} is the value of σ when the frame $O_g x'y'z'$ is created and $\boldsymbol{D}$ is a 3×1 displacement vector:

$$\boldsymbol{D} = -\boldsymbol{R}_{gc}\boldsymbol{P}_{og} \tag{7}$$

where $\boldsymbol{P}_{og}$ is the position of the origin O_g of the frame $O_g x'y'z'$ in the frame $O_c xyz$. Fig. 8 indicates the new relationship between the UAV and F in the frame $O_g x'y'z'$. For the guidance sub-phase, it has.

The velocity vector of the UAV in the frame $O_g x'y'z'$

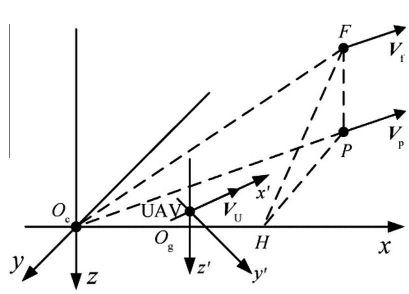

Fig. 7 Position relationship at the end of the correction sub-phase.

$$\boldsymbol{V}'_U = \boldsymbol{R}_{gc}\boldsymbol{V}_U$$

The position vector of F in the frame $O_g x'y'z'$

$$\boldsymbol{P}'_f = \boldsymbol{R}_{gc}\boldsymbol{P}_f + \boldsymbol{D} = [x'_f, y'_f, z'_f]^T$$

The velocity vector of F in the frame $O_g x'y'z'$

$$\boldsymbol{V}'_f = \boldsymbol{R}_{gc}\boldsymbol{V}_f$$

The iterative computation process for the guidance sub-phase is the same as that described in the correction sub-phase.

3.2. Formation phase

The formation phase is to consider how to keep the UAV and the tanker flying in a formation for the preparation of the docking of the refueling probe of the UAV with the drogue of the tanker. When the distance between the UAV and the tanker is less than a specified value, a velocity coordinate system $O_v x''y''z''$ is created as shown in Fig. 9. The frame $O_v x''y''z''$ is used to measure the target location for computing the control variable. Fig. 9 shows the position relation between the UAV and F in the frame $O_v x''y''z''$ during the formation phase. In order to guide the UAV to the formation point F and keep the same flight direction, a control acceleration a_n is designed to apply on the UAV with direction pointing to F'', which is a projection of formation point F on the $O_v y''z''$ plane in the velocity coordinate system as shown in Fig. 10. The magnitude of a_n is determined according to the coordinate value of F in the frame $O_v x''y''z''$ as

$$a_n = A\sin\delta \tag{8}$$

where A is a constant and δ is the angle between the UAV velocity and the relative position vector of F to the UAV.

Besides, the formation flight phase in AAR requires the speed of the UAV to be consistent with that of the tanker. For this reason, the control acceleration a_b (see in Fig. 10) along with the direction of the UAV speed should be utilized to control the speed of the UAV. The magnitude of a_b depends

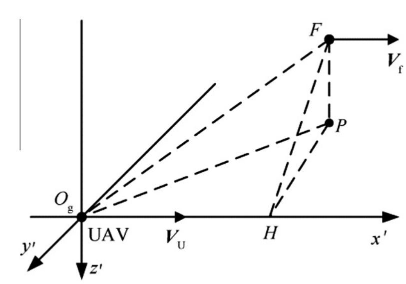

Fig. 8 New position relationship in $O_g x'y'z'$.

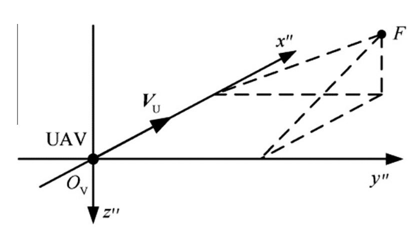

Fig. 9 UAV position relative to the formation point.

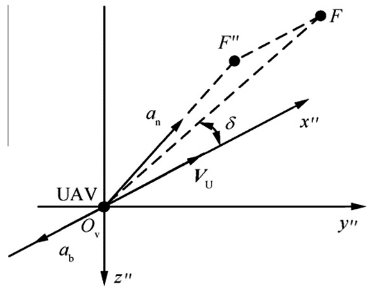

Fig. 10 Control direction of UAV.

on the relative distance between the UAV and F as well as their current speeds.

The flight time needed for the UAV to cover a distance of s can be calculated as

$$t = \frac{2s}{v_{\mathrm{U}} + v_{\mathrm{f}}}$$

where s is the arc trajectory for the UAV moving to F computed in the frame $O_{\mathrm{v}}x''y''z''$. The magnitude of the control acceleration a_{b} can be calculated by

$$a_{\mathrm{b}} = \frac{v_{\mathrm{f}} - v_{\mathrm{U}}}{t} = \frac{v_{\mathrm{f}}^2 - v_{\mathrm{U}}^2}{2s} \tag{9}$$

In summary, the rendezvous process for the UAV with the tanker can be described by the flow chart shown in Fig. 11.

4. Simulations and analysis

In order to verify the effectiveness of the ICGL for the rendezvous and formation maintaining problem in AAR, a simulation is performed here using the proposed ICGL by comparing with the NG approach presented in Ref. 25 to demonstrate the effectiveness of the ICGL.

In this simulation, assume that the initial conditions of the UAV and the tanker are as follows:Position vector of the UAV

$$\boldsymbol{P}_{\mathrm{U}}(t_0) = [x_{\mathrm{U}}(t_0), y_{\mathrm{U}}(t_0), z_{\mathrm{U}}(t_0)]^{\mathrm{T}} = [0, 0, 0]^{\mathrm{T}}\mathrm{m}$$

Velocity vector of the UAV

$$\boldsymbol{V}_{\mathrm{U}}(t_0) = \left[v_{\mathrm{U}x}(t_0), v_{\mathrm{U}y}(t_0), v_{\mathrm{U}z}(t_0)\right]^{\mathrm{T}} = [100, 0, 0]^{\mathrm{T}}\ \mathrm{m/s}$$

Position vector of the tanker

$$\boldsymbol{P}_{\mathrm{t}}(t_0) = [x_{\mathrm{t}}(t_0), y_{\mathrm{t}}(t_0), z_{\mathrm{t}}(t_0)]^{\mathrm{T}} = [5000, -3000, -1000]^{\mathrm{T}}\ \mathrm{m}$$

Velocity vector of the tanker

$$\boldsymbol{V}_{\mathrm{t}}(t_0) = \left[v_{\mathrm{t}x}(t_0), v_{\mathrm{t}y}(t_0), v_{\mathrm{t}z}(t_0)\right]^{\mathrm{T}} = [50, -40, 0]^{\mathrm{T}}\ \mathrm{m/s}$$

During the formation phase, the relative position of the UAV to the tanker is set as

$$\Delta\boldsymbol{d} = \left[\Delta d_x, \Delta d_y, \Delta d_z\right]^{\mathrm{T}} = [35, 35, 50]^{\mathrm{T}}\ \mathrm{m}$$

Simulations for the rendezvous and formation maintaining process of the UAV with the tanker are performed by using the ICGL and the NG methods, respectively. Fig. 12 shows the trajectories of the UAV approaching to the tanker in the rendezvous and formation maintaining process using the ICGL and the NG.

The control accelerations for the correction and guidance sub-phases are shown in Fig. 13. a_{c} and a_{g} is the acceleration in the correction sub-phase and guidance sub-phase, respectively. Using $E = \int_{t_0}^{t_{\mathrm{f}}} a^2 \mathrm{d}t$,[26] we can compute the energy consumptions $E_{\mathrm{ICGL}} = 1108.5$ for the ICGL and $E_{\mathrm{NG}} = 1270$ for the NG, respectively. Obviously, the UAV consumes less energy to accomplish the rendezvous process by using the ICGL than by using the NG.

The altitude change histories of the UAV during the rendezvous process are shown in Fig. 14 for the ICGL and the

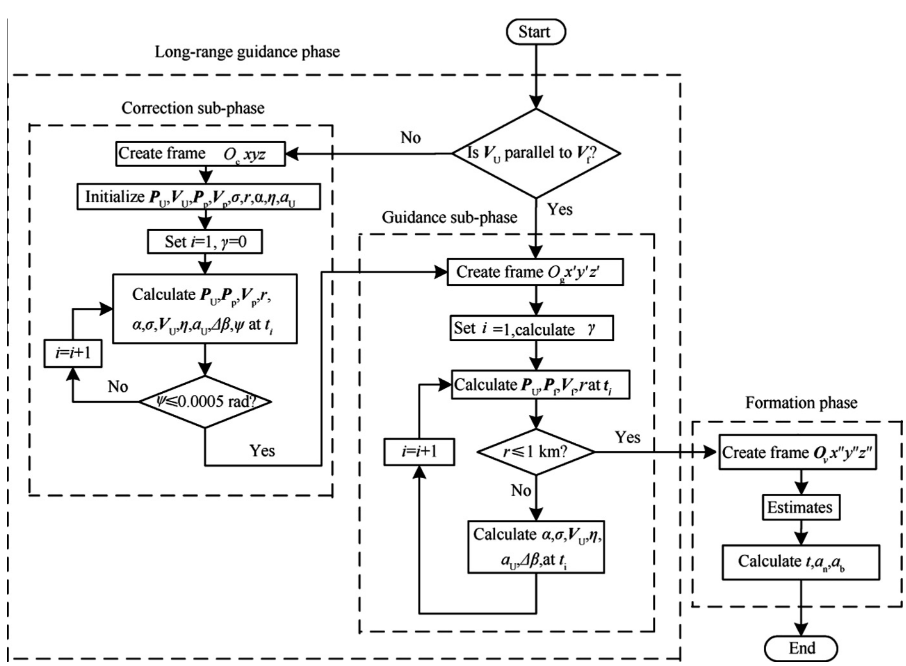

Fig. 11 Flow chart for the ICGL approach.

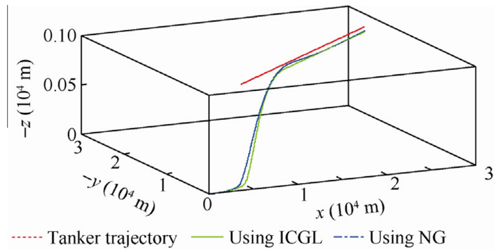

Fig. 12 Trajectories through the rendezvous process using ICGL and NG.

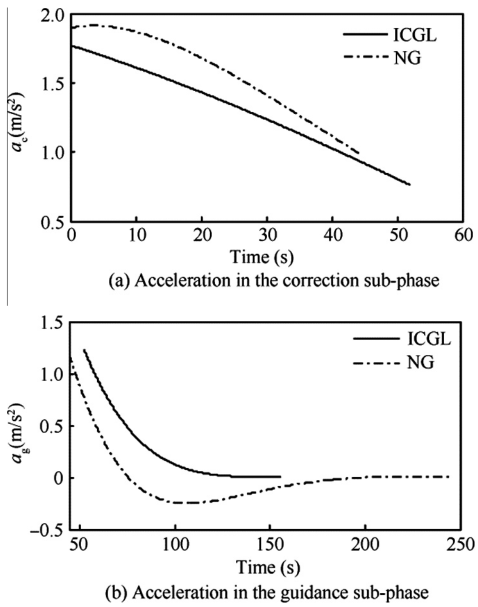

Fig. 13 Control accelerations in the correction sub-phase and guidance sub-phase.

NG. By comparison, it can be seen that, during the correction sub-phase, it takes 52 s for the UAV to complete its velocity direction adjustment using the ICGL and 44.2 s using the NG. For the guidance sub-phase, it takes 103.4 s to complete this process using the ICGL compared with 200.8 s using the NG. In general, it takes 217 s in total to accomplish the whole rendezvous process using the ICGL and 300 s using the NG. It is obvious that the proposed ICGL has better performance than the NG for the rendezvous problem.

Figs. 15 and 16 show the change histories of the distance and the velocity angle between the UAV and the tanker during the whole rendezvous process using the ICGL, respectively. It can be seen from Figs. 15 and 16 that the UAV eventually keeps a formation flight with the tanker. This indicates the effectiveness of the proposed ICGL method. Δb represents the distance between the UAV and the tanker in Fig. 15, $\Delta\theta$ represents the angle between the velocity vectors of the UAV and the tanker in Fig. 16.

To test the robustness of the proposed ICGL to wind disturbance, we add a step wind disturbance along the x-axis with amplitude of $a_{\mathrm{w}} = 2\ \mathrm{m/s^2}$ at the simulation time of 300 s in the formation maintaining phase as shown in Fig. 17. The

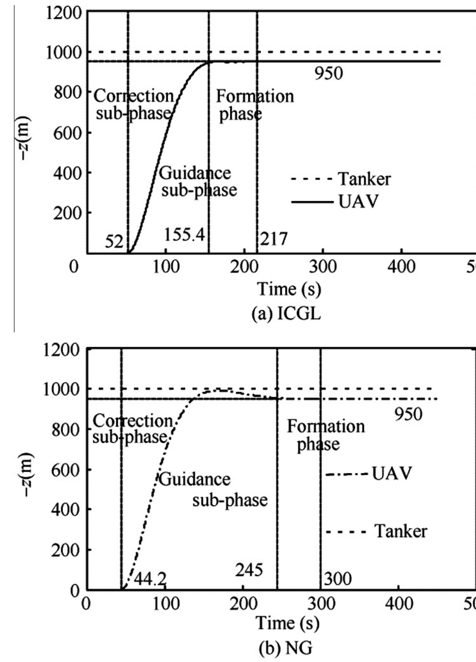

Fig. 14 UAV and tanker flight altitude change histories using ICGL and NG.

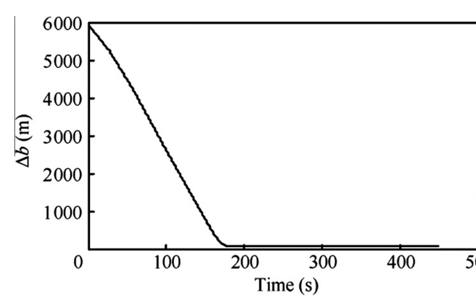

Fig. 15 Distance between UAV and tanker.

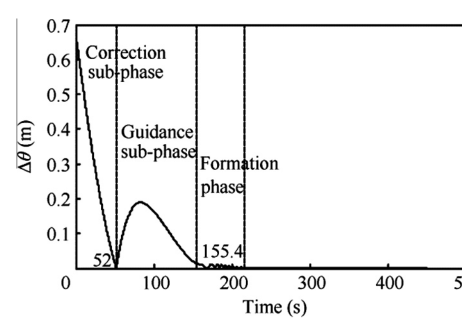

Fig. 16 Angle between the velocity vectors of UAV and tanker.

simulation result for the whole rendezvous process is shown in Fig. 18. Fig. 19 shows the deviations Δx and Δy of the UAV to the desired distance with the tanker in the x-axis and y-axis directions in the presence of wind disturbance. It can be seen

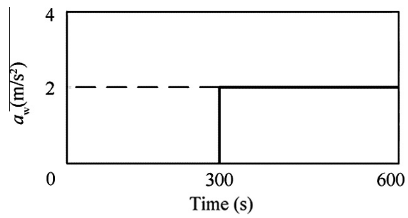

Fig. 17 A step wind disturbance.

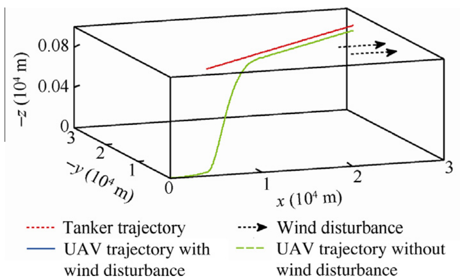

Fig. 18 Trajectories of the rendezvous process against wind disturbance.

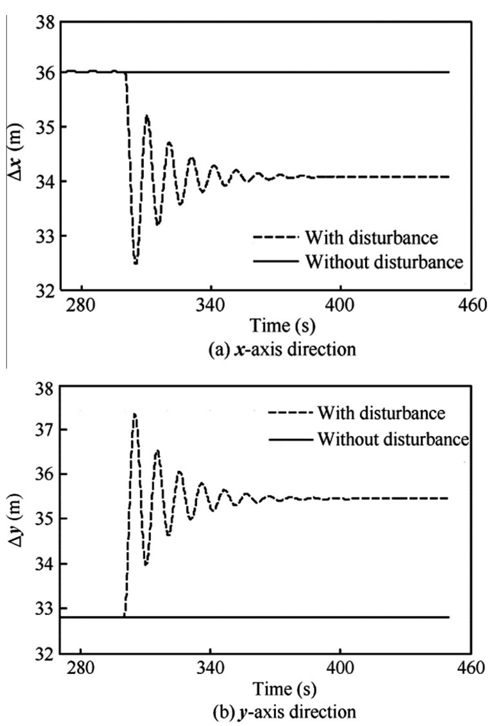

Fig. 19 Distance between UAV and tanker on.

that the steady state error is about 2 m in the x-axis direction and less than 3 m in the y-axis direction. Fig. 20 shows the change of the control acceleration a_d of the UAV under wind disturbance. The simulation result indicates that the proposed ICGL has good robustness against wind disturbance.

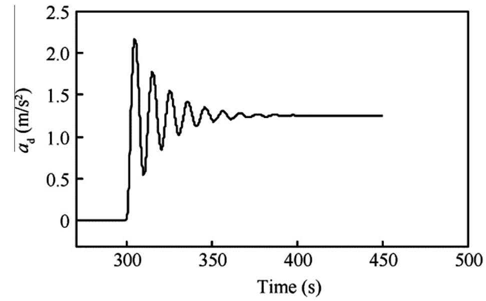

Fig. 20 Control acceleration of UAV under wind disturbance.

5. Conclusions

(1) A guidance approach of the ICGL addressing the rendezvous and formation problem for a UAV in AAR is presented in this paper. The ICGL divides the whole process into two phases: the long-range guidance phase and the formation phase, in which the long-range guidance phase is further divided into two sub-phases: the correction sub-phase and the guidance sub-phase.
(2) The ICGL solves the guidance problem of each phase and sub-phase in a two-dimensional space with the iterative method to obtain the control acceleration for the UAV.
(3) Simulation results demonstrate that the proposed ICGL is effective for the UAV to deal with the rendezvous and formation problem in AAR and is robust against wind disturbance.

Acknowledgements

We would like to thank the anonymous reviewers for their constructive comments on this manuscript. This study was partially supported by the National Natural Science Foundation of China (No. 61333004), partially by the Aeronautical Science Foundation of China (No. 20115868009), and partially by the open funding project of the State Key Laboratory of Virtual Reality Technology and Systems at Beihang University of China (No. BUAA-VR-13KF-01).

References

1. Luo DL, Lu TX, Wu SX. A survey on guidance laws for flight vehicle. *J Syst Simul* 2010;**22**(S1):16–20 [Chinese].
2. Guo J, Dong XM, Xu YJ, Liao KJ. Design of UAV autonomous controller for rendezvous in aerial refueling. *Contr Decis* 2010;**25**(4):567–71 [Chinese].
3. Liang X, Wang HL, Li DW, Lv WT. Three-dimensional path planning for unmanned aerial vehicles based on principles of stream avoiding obstacles. *Acta Aeronaut Astronaut Sin* 2013;**34**(7):1670–81 [Chinese].
4. Guelman M. A qualitative study of proportional navigation. *IEEE Trans Aerosp Electron Syst* 1971;**7**(4):337–43.
5. Tyan F. Capture region of a GIPN guidance law for missile and target with bounded maneuverability. *IEEE Trans Aerosp Electron Syst* 2011;**47**(1):201–13.
6. Lin CL, Li YH. Development of 3-D modified proportional navigation guidance law against high-speed targets. *IEEE Trans Aerosp Electron Syst* 2013;**49**(1):677–87.

7. Zhao SY, Zhou R, Wei C, Ding QX. Design of time-constrained Guidance Laws via virtual leader approach. *Chin J Aeronautics* 2010;**23**(1):103–8.
8. Yamasaki T, Balakrishnan SN, Takano H. Integrated guidance and autopilot design for a chasing UAV via high-order sliding modes. *J Franklin Inst* 2012;**349**(2):531–58.
9. Miao SQ, Cong BL, Liu XD. Adaptive sliding mode control of flexible spacecraft on input shaping. *Acta Aeronaut Astronaut Sin* 2013;**34**(8):1906–14 [Chinese].
10. Wang L, Li GC, Wang ZL, Jiao B. Sliding mode control of an under actuated quadrotor UAV. *J Harbin Eng Univ* 2012;**33**(10):1248–53.
11. Jing WX, Li CY, Qi ZG. Application of the 3D differential geometric guidance commands. *J Astronaut* 2007;**28**(5):1235–40 [Chinese].
12. Peng SC, Pan L, Han DP, Shen LC. A new 3D guidance law based on nonlinear method. *Acta Aeronaut Astronaut Sin* 2010;**31**(10):2018–25 [Chinese].
13. Li J, An HL, Xiang XJ, Shen LC. UAVs formation rendezvous method based on differential geometry and Lie group. *J Natl Univ Def Technol* 2013;**35**(6):157–64 [Chinese].
14. Li XS, Li X. Robust adaptive backstepping design for unmanned aerial vehicle formation guidance and control. *J Appl Sci* 2012;**30**(5):552–8 [Chinese].
15. Xia QY, Xu JF. A design of triaxial unmanned rotor aircraft and its adaptive flight control system. *Acta Aeronaut Astronaut Sin* 2013;**34**(3):495–508 [Chinese].
16. Luo YL, Yin CX. Study of small UAV control system based on fuzzy RBF neural network. *J Civil Aviat Flight Univ China* 2014;**25**(1):46–9 [Chinese].
17. Hassan GM, Yahya KM, Haq IU. Leader-follower approach using full-state linearization via dynamic feedback. *Proceedings of the International Conference on Emerging Technologies*; 2006 Nov 13–14; Peshawar, Pakistan; 2006. p. 297–305.
18. Linorman NHM, Liu HHT. Formation UAV flight control using virtual structure and motion synchronization. *Proceedings of the American Control Conference*; 2008 Jun 11–13; Seattle, WA, USA; 2008. p. 1782–7.
19. Karimoddini A, Lin H, Chen BM, Lee TH. Hybrid three-dimensional formation control for unmanned helicopters. *Automatica* 2013;**49**(2):424–33.
20. Han ZZ. An iterative guidance method for the large launch vehicle. *J Astronaut* 1983;**1**:9–21 [Chinese].
21. Fu Y, Chen G, Lu BG, Guo JF, Cui NG. A vacuum adaptive iterative guidance method of launch vehicle based on optimal analytical solution. *Acta Aeronaut Astronaut Sin* 2011;**32**(9):1696–704 [Chinese].
22. Song ZY. From accurate, precise to perfect-manned space promotes the development of guidance method on launch vehicle. *Aerosp Contr* 2013;**31**(1):4–10 [Chinese].
23. Xiao LX, Wang JP, Wang AM, Yang J. Optimal iterative guidance method based on required trajectory. *Aerosp Shanghai* 2012;**29**(3):1–5 [Chinese].
24. Chandler DC, Smith IE. Development of the iterative guidance mode with its application to various vehicles and missions. *J Spacecraft Rockets* 1967;**4**(7):898–903.
25. Park S, Deysty J, How JP. A new nonlinear guidance logic for trajectory tracking. *Proceedings of the AIAA Guidance, Navigation, and Control Conference and Exhibit*; 2004 Aug 16–19; Providence, Rhode Island, USA; 2004. p. 16–9.
26. Luo DL, Li YF, Wu WH, Shen CL. Terminal guidance law based on receding horizon control for homing missile. *J Nanjing Univ Aeronaut Astronaut* 2005;**37**(1):52–6 [Chinese].

Luo Delin received Ph.D. degree in navigation, guidance and control from Nanjing Universtiy of Aeronautics and Astronautics in 2006. He is presently an associate professor with the Department of Automation, School of Information Science and Technology, Xiamen University. His research interests include flight vehicle guidance and control, UAV cooperative control and decision making.

Xie Rongzeng received B.S. degree in automation from Wuhan University of Technology in 2010. Currently, he is a M.S candidate at the Department of Automation, Xiamen University. His research interests include UAV guidance and cooperative control.

Duan Haibin received Ph.D. degree in control theory and control engineering from Nanjing Universtiy of Aeronautics and Astronautics in 2005. He is currently a professor with the School of Automation Science and Electrical Engineering, Beihang University. His research interest include flight control, autonomous control of multiple aerial vehicles, computational intelligence.